NOSC TD 1244

NAVAL OCEAN SYSTEMS CENTER San Diego, California 92152-5000

NOSC TD 1244

Technical Document 1244
March 1988

Detector Evaluation for Optical Signals

H. Roehrig
M. P. Browne

University of Arizona
Tucson, Arizona

NAVAL OCEAN SYSTEMS CENTER

San Diego, California 92152-5000

E. G. SCHWEIZER, CAPT, USN
Commander

R. M. HILLYER
Technical Director

ADMINISTRATIVE INFORMATION

Contract N66001-85-D-0203 was carried out at the Optical Sciences Center at the University of Arizona, Tucson, AZ under the direction of the San Diego State University Foundation. Funding was provided by the Defense Advanced Research Projects Agency, Code DARP-STO, Arlington, VA.

Released by
R. P. Schindler, Head
Electro-Optic Systems Branch

Under authority of
M. S. Kvigne, Head
Space Systems Division

PK

REPORT DOCUMENTATION PAGE

1a. REPORT SECURITY CLASSIFICATION UNCLASSIFIED	1b. RESTRICTIVE MARKINGS
2a. SECURITY CLASSIFICATION AUTHORITY	3. DISTRIBUTION/AVAILABILITY OF REPORT
2b. DECLASSIFICATION/DOWNGRADING SCHEDULE	Approved for public release; distribution is unlimited.
4. PERFORMING ORGANIZATION REPORT NUMBER(S)	5. MONITORING ORGANIZATION REPORT NUMBER(S) NOSC TD 1244

6a. NAME OF PERFORMING ORGANIZATION Optical Sciences Center	6b. OFFICE SYMBOL (if applicable)	7a. NAME OF MONITORING ORGANIZATION Naval Ocean Systems Center
6c. ADDRESS (City, State and ZIP Code) University of Arizona Tucson, AZ 85721		7b. ADDRESS (City, State and ZIP Code) Code 844 San Diego, CA 92152-5000
8a. NAME OF FUNDING/SPONSORING ORGANIZATION Defense Advanced Research Projects Agency	8b. OFFICE SYMBOL (if applicable) DARP-STO	9. PROCUREMENT INSTRUMENT IDENTIFICATION NUMBER N66001-85-D-0203
8c. ADDRESS (City, State and ZIP Code) Arlington, VA 22209		10. SOURCE OF FUNDING NUMBERS

PROGRAM ELEMENT NO.	PROJECT NO.	TASK NO.	AGENCY ACCESSION NO.
62301E	X1879		DN687623

11. TITLE (include Security Classification)

Detector Evaluation for Optical Signals

12. PERSONAL AUTHOR(S)

Hans Roehrig and Michael P. Browne

13a. TYPE OF REPORT	13b. TIME COVERED	14. DATE OF REPORT (Year, Month, Day)	15. PAGE COUNT
Final	FROM Jun 1986 TO Sep 1986	March 1988	36

16. SUPPLEMENTARY NOTATION

17. COSATI CODES			18. SUBJECT TERMS (Continue on reverse if necessary and identify by block number)
FIELD	GROUP	SUB-GROUP	

19. ABSTRACT (Continue on reverse if necessary and identify by block number)

The primary tasks associated with this contract were characterization and calibration of an RCA 8852 photomultiplier tube and a Varo image intensifier. The photomultiplier was characterized by its spectral response, absolute sensitivity, quantum efficiency, scan uniformity, dark current vs temperature, pulse-height distribution, and noise figure. The Varo intensifier was characterized by its response as a function of bias voltage both in the dark and while irradiated by an LED light source. This final report discusses the tests we performed and compares them with data in the open literature and with data obtained by means of private communication from other researchers in the field. "Optical Signal Amplification," by Richard H. Cromwell of the Seward Observatory at the University of Arizona is Apprendix A to this report.

20. DISTRIBUTION/AVAILABILITY OF ABSTRACT	21. ABSTRACT SECURITY CLASSIFICATION
☐ UNCLASSIFIED/UNLIMITED ☒ SAME AS RPT ☐ DTIC USERS	UNCLASSIFIED

22a. NAME OF RESPONSIBLE INDIVIDUAL	22b. TELEPHONE (include Area Code)	22c. OFFICE SYMBOL
Richard D. Anderson	(619) 553-3723	Code 844

DETECTOR EVALUATION FOR OPTICAL SIGNALS

This report covers activities authorized under US Navy Contract Number N66001-85-D-0203 related to Task One, performed by the Optical Sciences Center from August 26, 1986, to September 30, 1986

Central to our work was the analysis of an RCA 8852 photomultiplier tube (PMT), received from Dr. Sam Green of the McDonnell-Douglas Corporation. We also worked on an image intensifier, supplied by Bill Flynt of the Varo Corporation.

For the RCA 8852, the emphasis was on:

- Quantum efficiency as a function of wavelength
- Relative responsivity as a function of position over the useful area of the photocathode
- Anode current as a function of temperature
- Dark electron pulse-height distribution

In particular, it was important to evaluate the dark current of the RCA 8852 PMT as a function of temperature. Because of its high dark current at room temperature, it is impossible to obtain single electron pulse-height distributions with our system, which is designed for a maximum event rate of $r_{ev} = 3.3 \times 10^4$ events per second. The event rate of the 8852 at room temperature and -1600 V bias is around 3×10^5 events per second.

With respect to the Varo intensifier, the emphasis was on light output (or quantum gain) as a function of the applied voltage. To better characterize this device, it was necessary to get a feel for its "dead" voltage V_0 and its "linearity" expressed by the parameter n. We approached this by determining the light output as a function of the applied voltage, both when the photocathode is in the dark and when it is illuminated by our light-emitting-diode (LED) light source.

These tests are detailed in the following paragraphs.

A. Quantum Efficiency and Absolute Sensitivity of the RCA 8852 Photomultiplier Tube

To use the RCA 8852 PMT as a reference tube, the calibration procedure had to determine its absolute spectral response, which necessitated a thorough re-examination of the calibration facility. This facility, under the direction of Dr. Richard Cromwell of Steward Observatory, consists of a light source of known output, a very stable power supply for the

lamp, a filter wheel, a set of calibrated interference filters, a set of calibrated reference photocathodes, and a data-recording system consisting of an electrometer and a HP-41 caiculator to control the electrometer and gather data. The center wavelength of the filters (and hence the wavelength regions of measurement) are as follows: 298.9 nm, 313.0 nm, 350.0 nm, 380.8 nm, 406.4 nm, 425.0 nm, 497.4 nm, 550.0 nm, 650.0 nm, 750.9 nm, 795.0 nm, 853.0 nm and 901.9 nm.

From records of the calibrated photocathodes kept since 1980, we could track their degradation and select the best photocathodes to use as reference standards. The four reference photocathodes came from Hamamatsu, RCA, ITT, and Varo. In the wavelength region between 350 nm and 500 nm, we found that the photocathodes were stable to ±1%. In the ultraviolet, the Varo tube has no appreciable response, the Hamamatsu and the ITT are stable to within 2%, and the RCA seems to have increased its response by about 8%. For wavelengths longer than 500 nm we found that all of the photocathodes except the Hamamatsu had decayed somewhat. The Varo tube had decayed substantially, the RCA tube somewhat less, and the ITT tube still less, but all three were unstable enough at the long wavelengths of interest to preclude their being considered reference standards.

The Hamamatsu was chosen as the reference photocathode; its uncertainties at the longer wavelength filters are as follows:

+0%, -10% at 901.9 nm and 853 nm
+0%, -5% at 750.9 nm and 795 nm
+0%, -3% at 650 nm
±1% at 550 nm.

Interesting to note is that in Dr. Cromwell's collection of photocathodes, every tube measured thus far over a 6.5-yr period has decayed somewhat in the longer wavelength region (with the exception of the Hamamatsu) including the most stable (a Proxitronic 3861). The worst tube (Varo #28687) has decayed 77% in 4.75 years (or 16% per year) at 901.9 nm.

We next measured the response of the RCA 8852 photocathode alone to get the absolute sensitivity. This measurement was performed both at room temperature and cooled to -50°C (this temperature is nominal, with no real way to measure it accurately; we merely wanted to compare the two modes of operation). The PMT response is shown in Fig. 1. The graph reveals two interesting facts: 1) poor response at long wavelengths and 2) a response at longer wavelengths which worsens somewhat with cooling. After correcting the measured quantum efficiency for the non-uniform response of the photocathode (averaging over the whole photocathode as discussed in Section B) the quantum efficiency at 853 nm is 1.02% uncooled and 0.54% cooled. The uncooled measurement compares favorably with that made

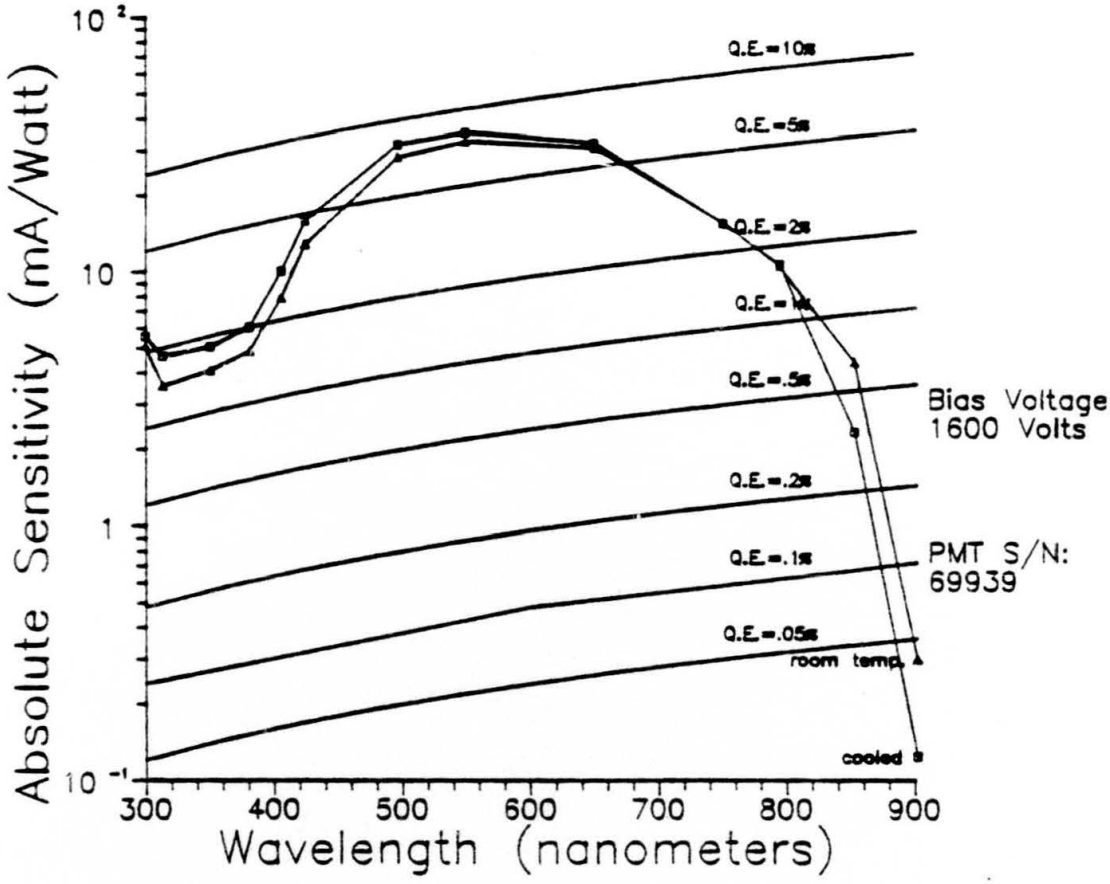

Fig. 1. Absolute sensitivity of RCA 8852 PMT measured both at room temperature and cooled.

by Dr. Sam Green in July, 1985, when he measured a quantum efficiency of 0.94%.[1] At 902 nm we measured a quantum efficiency of 0.082%. Dr. Green measured a quantum efficiency of 0.12% at a wavelength of 894 nm. Since we did not measure the photocathode uniformity at 894 nm, direct comparison of the quantum efficiency at longer wavelengths is not possible; but we feel that the rapidly decreasing tube response at longer wavelengths indicates that given Dr. Green's measurement at 894 nm, ours at 902 nm is not unreasonable.

The decreasing quantum efficiency at lower temperatures is most likely because at the longer wavelengths, photons may just have enough energy to create a photoelectron (possibly with the assistance of a phonon), and therefore lowering the device temperature will reduce the amount of phonons present, making fewer phonon-assisted transitions possible.

B. Spatial Uniformity of the Photocathode Sensitivity

When measurements of the absolute spectral response of the photomultiplier were made, we also made a one-dimensional scan through the center of the photomultiplier's

photocathode and measured the photocathode current for various wavelengths of light. The results of this test are shown in Fig. 2. Notice that the response at 4250 Å is still quite good, but as we move out toward longer wavelengths, the relative response is very non-uniform. Interesting to note is that the measurements of the tube response were made approximately across the center of the photocathode, which is also the region of least sensitivity at the longer wavelengths. This would seem to indicate that the response as given by Fig. 1 would not convey an accurate indication of the overall photocathode sensitivity, and that the overall sensitivity would be somewhat larger. To take this into account in our measurements of the quantum efficiency at longer wavelengths we assumed that the response was radially symmetric. (It is not, but this probably is not too bad an assumption.) We then averaged the response over the entire scan and also over just the region of irradiation for the quantum efficiency measurements; then we ratioed these two averages as a correction factor for the measured quantum efficiency to extrapolate the quantum efficiency as would be measured over the entire photocathode for the two wavelengths 853 and 902 nm.

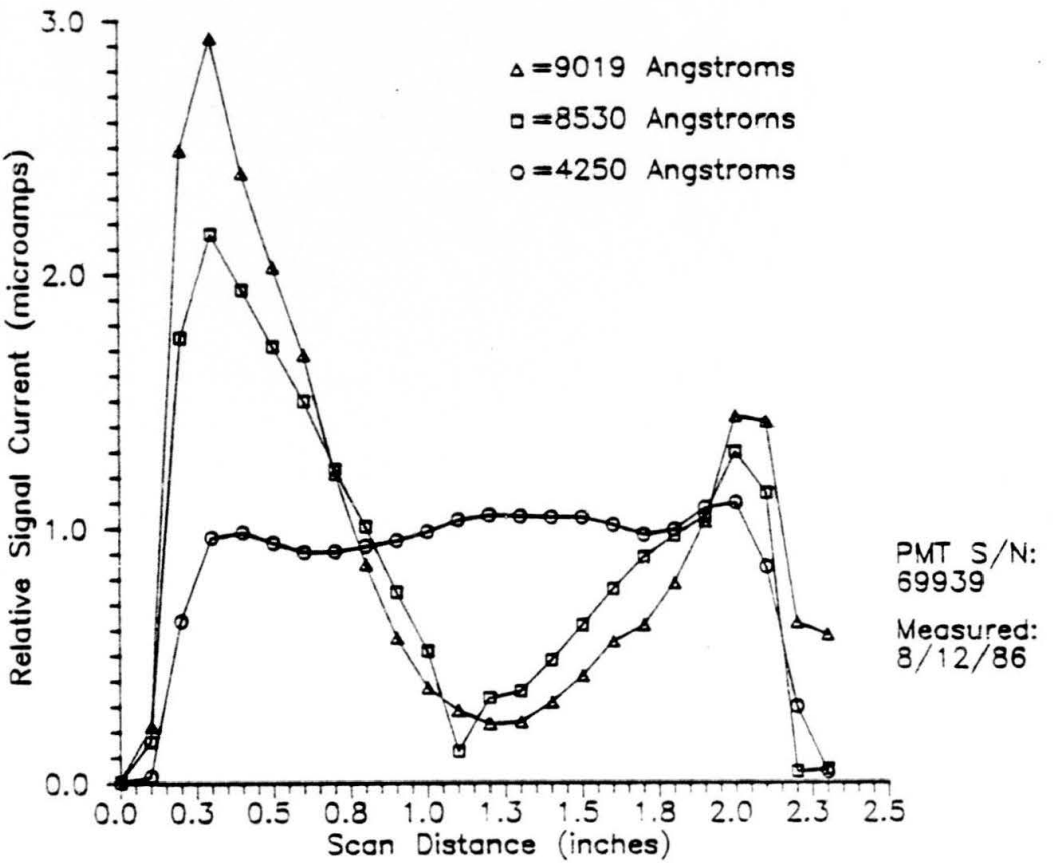

Fig. 2. Uniformity scan across the photocathode of an RCA 8852 PMT. A 0.24-in. scanning spot size was used.

Curious about the rather large variations in photocathode response as a function of position, we discussed our data with Dr. Green. It was his opinion that large variations in photocathode response are typical and are especially prevalent at longer wavelengths, where the lower energy of the photon and thus of its created photoelectron means that even the smallest defect in the photocathode will have an effect on conversion efficiency by reducing the energy of the less energetic photoelectrons so that they can no longer escape the photocathode material and become free photoelectrons.

C. PMT Anode Dark Current vs Temperature

Testing the RCA 8852 revealed that the dark current is much higher at room temperature than the dark current of the RCA 8850 (6×10^{-8} A compared to 2×10^{-11} A) at the same bias voltage of -1600 V and after both tubes had been conditioned in the dark with bias voltage on for at least 48 hr. Because of the high dark current, the 8852 was often operated at reduced temperatures by installing it in a Products for Research model TE-254-TS-RE-ND refrigerated photomultiplier housing. This housing consists of a pump/refrigeration unit and a housing unit/heat exchanger, connected by a flexible hose which carries the Freon coolant. The unit has a dial which nominally selects the temperature at the photocathode and is calibrated in six steps: 0°C, -10°C, -20°C, -30°C, -40°C, and -50°C. We were interested in measuring the reduction in dark current for a given decrease in operating temperature. The tube was biased to -1600 V and the dark current was measured at the anode using a Keithley Model 602 Electrometer. The results of this experiment are shown in Fig. 3.

As expected, there is a strong dependence of the dark current on the absolute temperature. For the specific example of -1600 V bias voltage, the anode current reduces from 4.2×10^{-8} A to about 1.5×10^{-10} A, which is more than 2 orders of magnitude. This is both expected and predictable from the Richardson equation, which gives the dependence of the electron emission of a surface on temperature (making the appropriate assumptions for the bandgap of the material).[2]

$$j = \frac{4\pi emk^2T^2}{h^3} e^{((E_a-E_g)/2)/kT} \qquad (1)$$

where:

j = thermionic current density
e = electron charge
m = electron mass
k = Boltzmann's constant
h = Planck's constant
E_a = electron affinity
E_g = bandgap

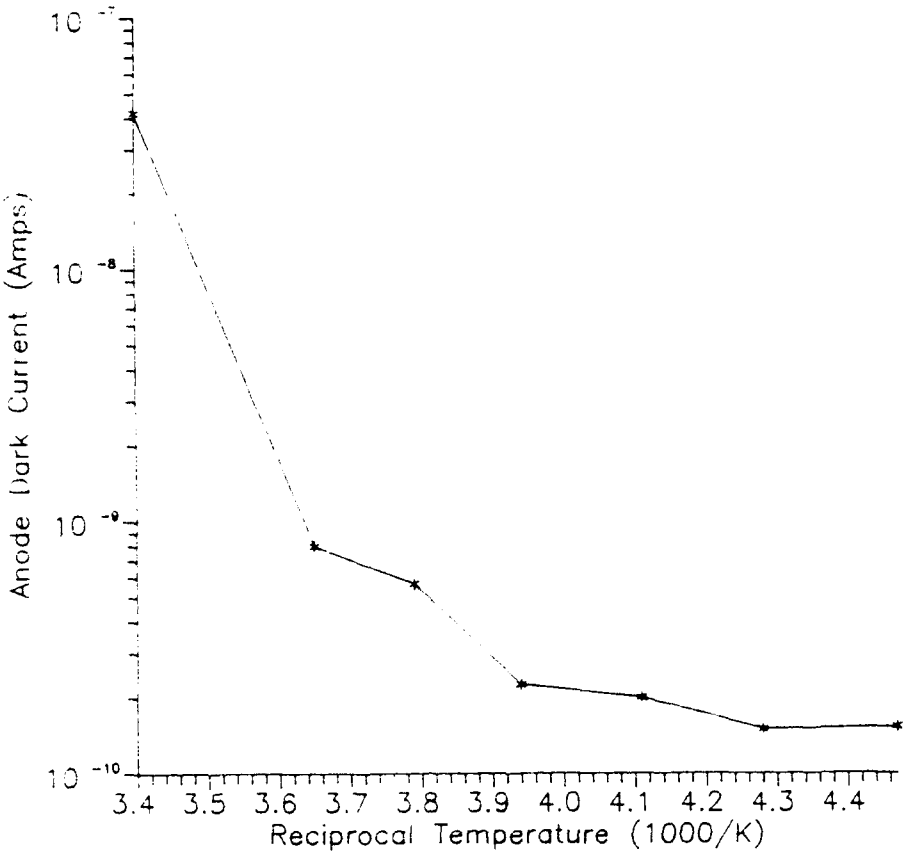

Fig. 3. Anode dark current of RCA 8852 measured as a function of temperature.

or, if the constants are given in mks units, (1) becomes

$$j = 1.2\times10^{6}T^{2}e^{((E_a-E_g)/2)/kT} \quad . \tag{2}$$

This decrease in dark current with decreasing temperature also agrees with the findings of other researchers (Dr. Richard Cromwell) and with the literature.[3] An example for the latter is Fig. 16 of the RCA Photomultiplier Handbook[4] which is reproduced in this report as Fig. 4. Our curve appears to bottom out because the temperature feedback mechanism in the cooler is not extremely reliable for the following reasons: 1) the temperature sensor makes no contact with the photomultiplier photocathode and, 2) the only indication that the cooler has actually "cooled down to temperature" is a cycling of the refrigeration unit, which could also be attributable to mechanical considerations alone (i.e., a finite on/off time to prevent frosting of the input window).

D. Single Dark Electron Pulse-Height Distributions

Single dark electron pulse-height distributions can only be made if the emission rate of dark electrons (thermionic electrons) r_{ei} at the PMTs photocathode is at least an order of

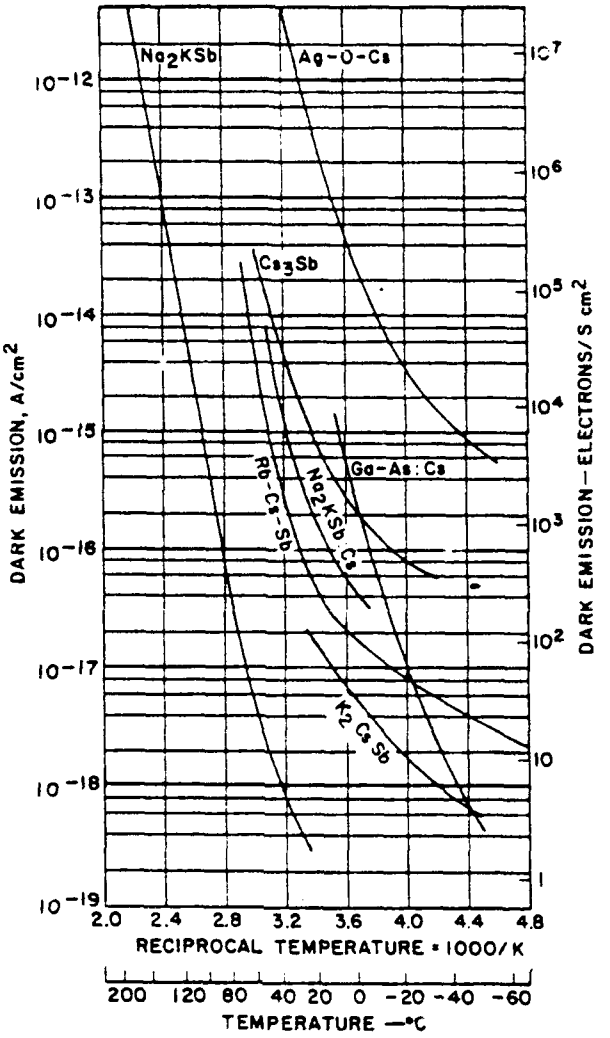

Fig. 4. Variation of thermionic-emission current density from various photocathodes used in photomultiplier tubes as a function of reciprocal temperature. Thermionic emission multiplied by the gain of the photomultiplier is a principal source of anode dark current. (Ref. 2)

magnitude (if not two orders) lower than the highest event rate r_{ev} the instrumentation can handle:

$$r_{el} << r_{ev} \quad . \tag{3}$$

We commonly use an integrator described in detail in the final report for Contract N66001-85-C-0118.[5] Its shortest integration time is $t_i = 30\mu s$ and, consequently, its highest event rate r_{ev} is $r_{ev} = 1/t_i = 1/(30\ \mu s) = 3.3\times10^4$ events per second.

The condition of Eq. (3) can be achieved for the RCA 8852 PMT by cooling to -50°C (nominal). At this temperature, the anode dark current is about 2×10^{-10} A. Assuming a gain of 9×10^5 for -1600 V, (a value which can be found from the RCA data sheets on the

RCA 8852),[6] the dark electron rate at the cathode is r_{el} = 1.4×10^{5} electrons/second. This value is easily matched by the event rate r_{ev} = 3.4×10^{4} events per second.

Figure 5 shows a single dark electron pulse-height distribution taken with the RCA 8852 at a temperature of about -50° C. It was obtained using a PMT voltage of -1600 V, a load resistor of 21.4 kΩ, an integrator gain of 98647 sec^{-1}, a preamp gain setting of 500, and an MCA sensitivity of S_{MCA}=256 channels/volt. The integrator was operated in the internally triggered mode. Notice that the distribution peak is at channel number 80.

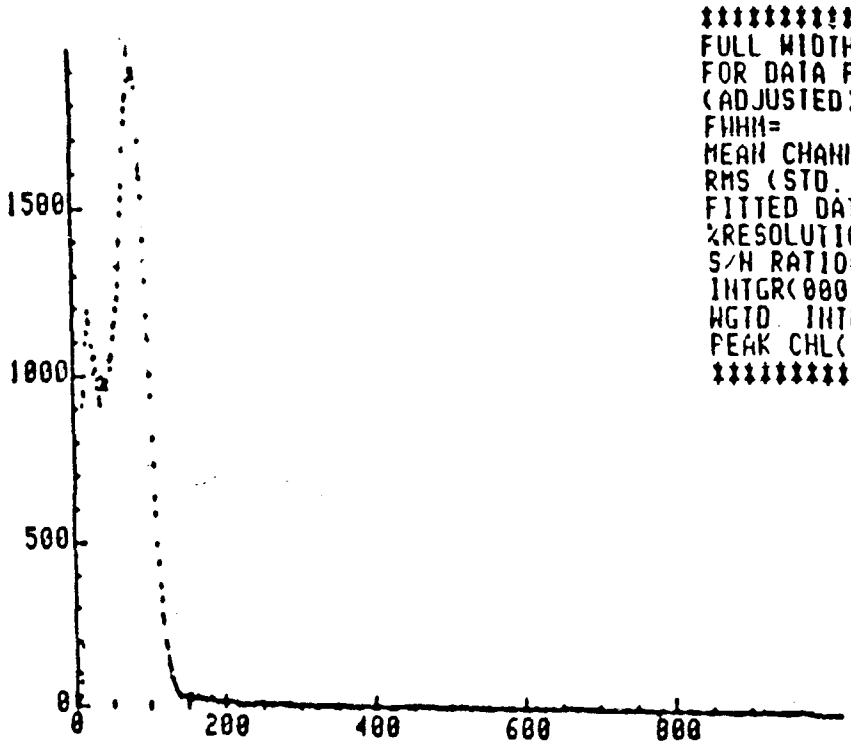

Fig. 5. Pulse-height distribution for an RCA 8852 PMT at -1600 V bias and cooled to -50°C (nominal).

The experimental setup is similar to that shown schematically in Figs. 6 and 7. Notice that the setup includes a light source (LED) which of course is not used for measuring single dark electron pulse-height distributions. Rather, it is only used if measurement of single signal electron pulse-height distributions (which incidentally should not be different from the single dark electron distributions) is desired. Figure 7 describes the operation of the integrator and provides a formula by which the photomultiplier's gain can be calculated from the characteristics of the distribution displayed by the multichannel analyzer (MCA). This equation is repeated here in a slightly modified form:

$$G = \frac{N_{ch} \cdot R_I \cdot C_I}{S_{MCA} \cdot G_A \cdot R_I \cdot e} \qquad (2)$$

where:

$1/(R_I \cdot C_I)$ = "gain of the integrator" [s^{-1}]

G_A = voltage gain of the preamplifier

R_I = load resistor [Ω]

e = electronic charge [coulombs]

S_{MCA} = sensitivity of the MCA [channels/V]

N_{ch} = channel number of particular characteristic of distribution.

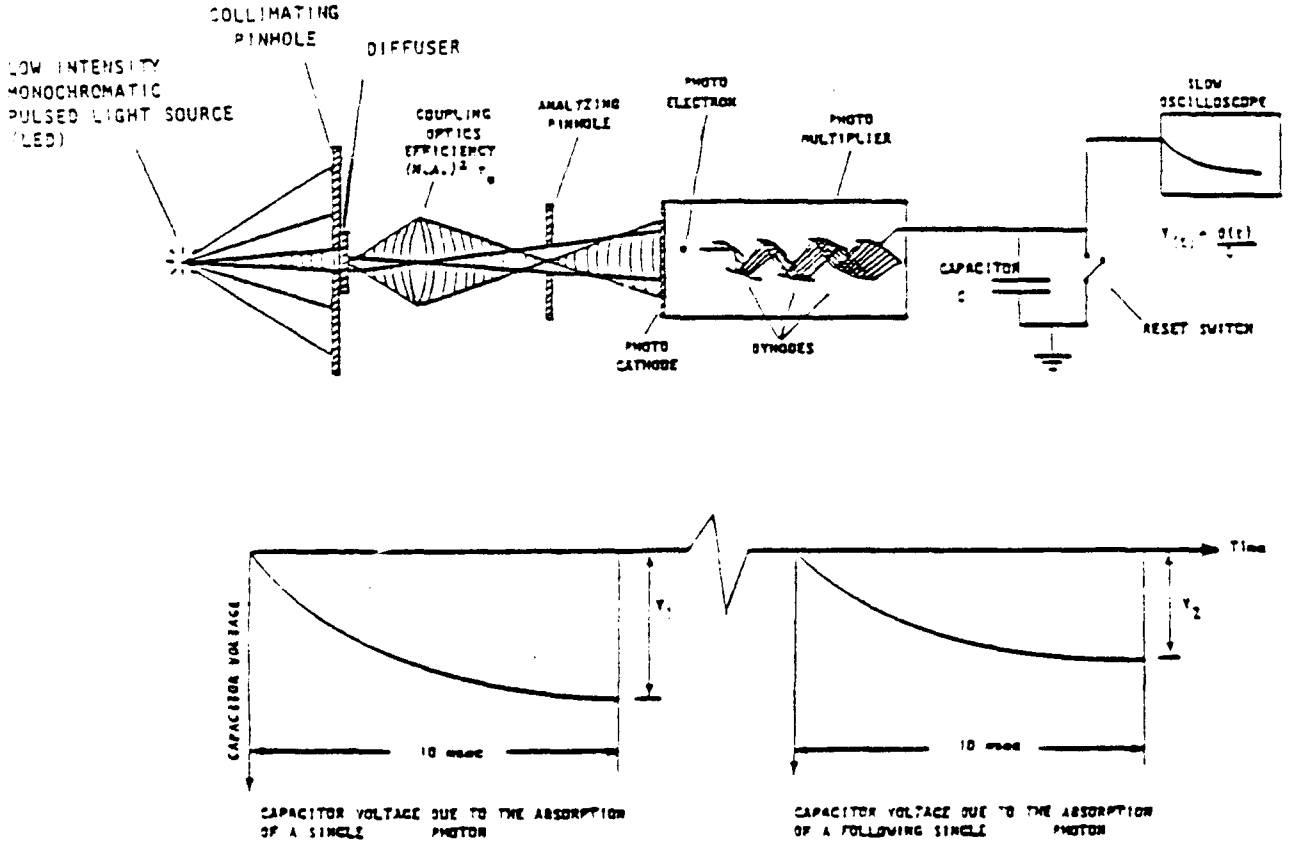

Fig. 6. Schematic illustrating the measurement of photoelectron pusle-height distribution of a photomultiplier using an analog integrator (capacitor with a reset switch) and a pulsed light source (LED).

Assuming for the moment that the distribution feature of interest is the distribution peak (one could also argue for the use of the distribution mean, weighted mean, median,

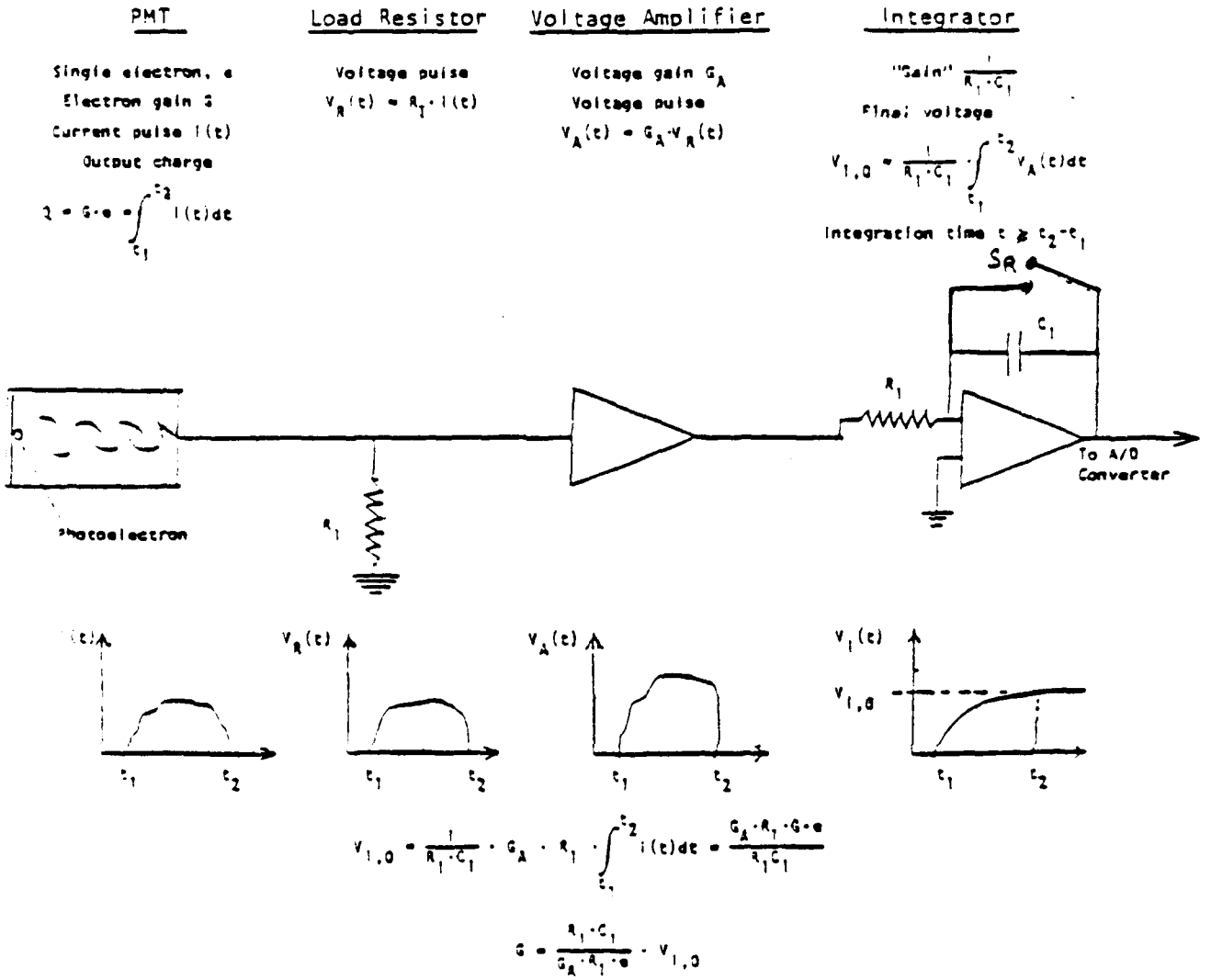

Fig. 7. The measurement of a photomultiplier's gain G from the integrator's voltage V for a PMT charge pulse attributable to one photoelectron (single electron pulse).

etc.; this subject has not been specifically addressed yet, and we are open for suggestions), the gain of the PMT is estimated to be 1.85×10^6. This gain value compares favorably with the value of 9×10^5, which is quoted as being typical by the RCA data sheet for the 8852.[6]

Of particular interest to this program is the determination of the noise factor, a characteristic which determines the amount of noise added by the detector (excess noise) to the noise inherent in the photon flux from the scene. As was outlined in the Final Report for Project N66001-85-C-0118,[7] the noise factor k is found from the mean μ_S and the

standard deviation σ_S of the single electron distribution according to:

$$k = \frac{\mu_S^2 + \sigma_S^2}{\mu_S^2} . \tag{5}$$

Using the values found in the above distribution, we find a value of 2.29 for the noise factor which seems to be reasonable.

It is interesting to relate the number of counts N_{CO} (total integrated counts = 139261) recorded during the duration T_e of the experiment (which was 2000 s) to the observed anode dark current i_A. Assuming that every dark electron emitted by the cathode leads to a recordable event (has enough amplitude to exceed the integrator's internal trigger threshold and therefore increment a channel in the multichannel analyzer) then the count rate r_{MCA} at the MCA should be matched by the dark electron rate r_{el} at the PMT's cathode or the dark electron rate $r_{el,a}$ at the PMT's anode divided by the PMT's gain G_{PMT}:

$$r_{MCA} = \frac{N_{CO}}{T_e} = \frac{r_{el,A}}{G_{PMT}} = \frac{i_A}{G_{PMT} \cdot e} = r_{el} \tag{6}$$

For this experiment, r_{MCA} = 68.8 counts/s while r_{el} = 69.3 counts/s, an error of only 0.7% !

Finally, an attempt was made to estimate the energy resolution, which is conventionally the ratio of the FWHM to the peak channel. We found a value of 70%, which is close to the value of 60% found in the RCA 8852 data sheet.[6]

Table 1 is a listing of some pertinent performance data on the RCA 8852 as measured by us and compared with data from the data sheets or other sources.

E. Varo Intensifier Light Output and Gain vs Bias Voltage

Image intensifiers of the Generation I type operate on the principle of cathode luminescence for the generation of gain. Here electrons emitted by the cathode are accelerated to a high kinetic energy $E_{kin} = 1/2\ mv^2 = eV$, where V equals the applied voltage. A major portion of this kinetic energy is used for excitation of electrons from the valence band to the conduction band of the phosphor material. Most of these excited electrons then give up their energy by returning to the valence band by means of energy levels in the forbidden band involving radiative transitions as shown schematically in Fig. 8. Unfortunately, however, not all the kinetic energy is used for the generation of light. It turns out that the electrons lose some energy in penetrating "dead" layers like the typical

Table 1. Pertinent performance data on the RCA 8852.

Quantity	Measured	From PMT Data Sheets
PMT voltage	-1600 V	—
Dark current @ -1600V	2.05×10^{-11} amps	2.0×10^{-8} amps @ 22°C
Count rate from dark current	69.3 counts/s	—
No. of counts from weighted integral	139261	—
Acquisition time	2,000 s	—
Observed count rate	68.8 counts/s	—
Peak Channel No.	80	—
Mean Channel No.	82.66	—
Standard Deviation	93.734	—
Current Gain @ -1600 V	1.85×10^{6}	8.5×10^{5}
Noise Factor (k)	2.29	1.87 - 1.94*
FWHM	56	—
Energy Resolution	70%	60%
Quantum Efficiency @ 852 nm	1.02%	0.94%*
Quantum Efficiency @ 894 nm	—	0.12%*
Quantum Efficiency @ 901 nm	0.082%	—

* From measurements made by Dr. Sam Green.[1]

aluminum backing of the phosphor. This energy is characterized by the so-called dead voltage V_0. Other losses are accounted for by the energy conversion efficiency η_{En}.

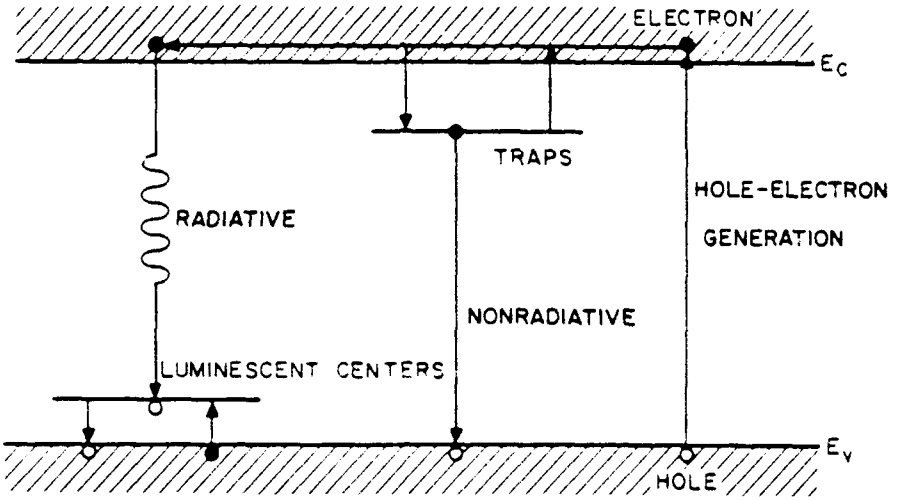

Fig. 8. Representation of radiative and nonradiative recombinations.

The number n_p of light photons emitted per photoelectron can be estimated from the effective kinetic energy $E_{kin,eff} = E_{kin} - eV_0$, the energy E_p of the emitted light photon, and the energy conversion efficiency η_{En}:

$$n_p = \eta_{En} \cdot \frac{E_{kin,eff}}{E_p} = \eta_{En} \cdot \frac{E_{kin} - eV_0}{E_p} . \tag{7}$$

Of particular interest is the dependence of η_{En} or n_p on the applied voltage. This can be estimated from the light output as a function of the accelerating voltage. The literature on cathode luminescence reports a general dependence as described in Eq. (8).[7]

$$L = k\,(V - V_0)^n \tag{8}$$

Here k is a constant of proportionality

V is the applied voltage

V_0 is the dead voltage

n is a constant which can take on values of from 1 to 3.[8]

Figure 9 is a linear representation of Eq. (8) for V_0 = 2 kV and n = 1. Figure 10 is a double logarithmic representation of Eq. (8) for V_0 = 3 kV, 5 kV, and 7 kV, and for n = 1.

Of particular importance were the particular values of V_0 and n for the phosphor in the Varo tube.

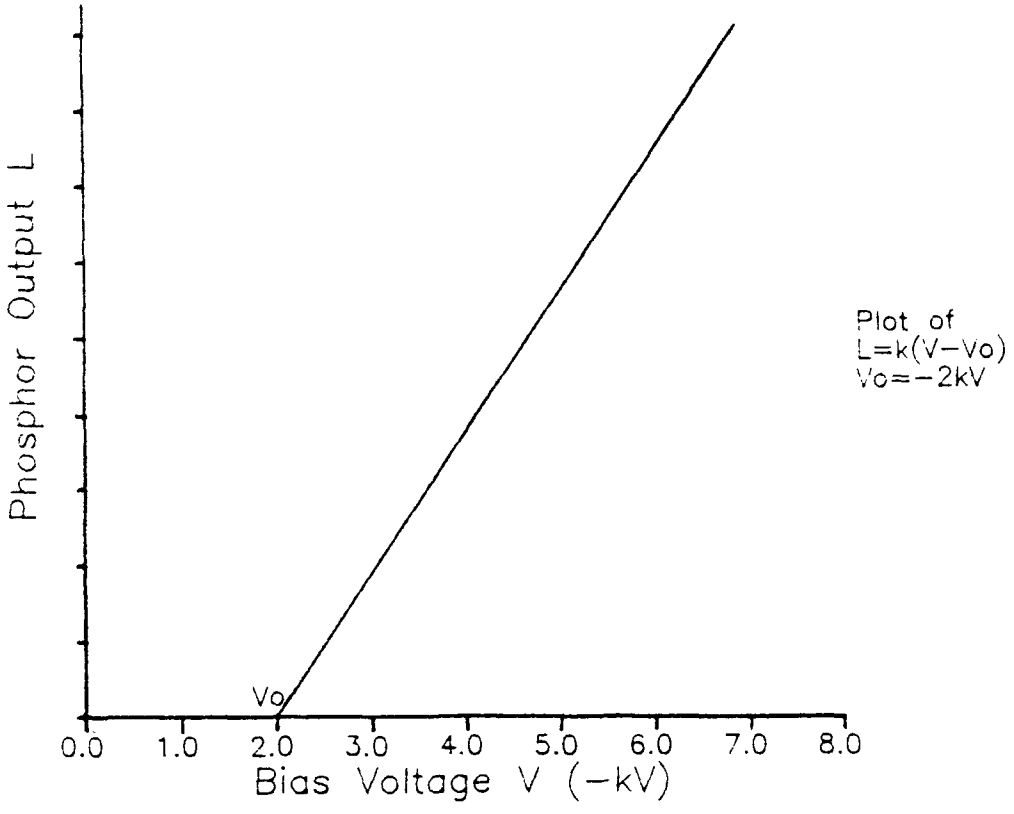

Fig. 9. Linear plot of phosphor light output as a function of applied voltage for V_0 = -2 kV and n = 1.

The experimental setup is shown schematically in Fig. 11. Notice that this is the setup which we normally use for measurements of the pulse-height distributions of image intensifiers which are basically AC type measurements. However, the system is easily modified by insertion of an electrometer into the anode circuit of the PMT to measure its DC anode current which then is a measure of the intensifier's light output.

Figure 12 shows on a log-log plot the output of the Varo image intensifier versus bias voltage, both in the dark and while irradiated. The output of the image intensifier was measured with an RCA 8850 photomultiplier tube coupled optically to the image intensifier using a high numerical aperture (NA = 0.95 in air) 100X microscope objective. The dark current for the photomultiplier was 2.1×10^{-11} A, and this value was subtracted from the anode current values while measuring the image intensifier. A more familiar plot may be the linear plot of the image-intensifier output vs bias voltages, which is shown in Fig. 13.

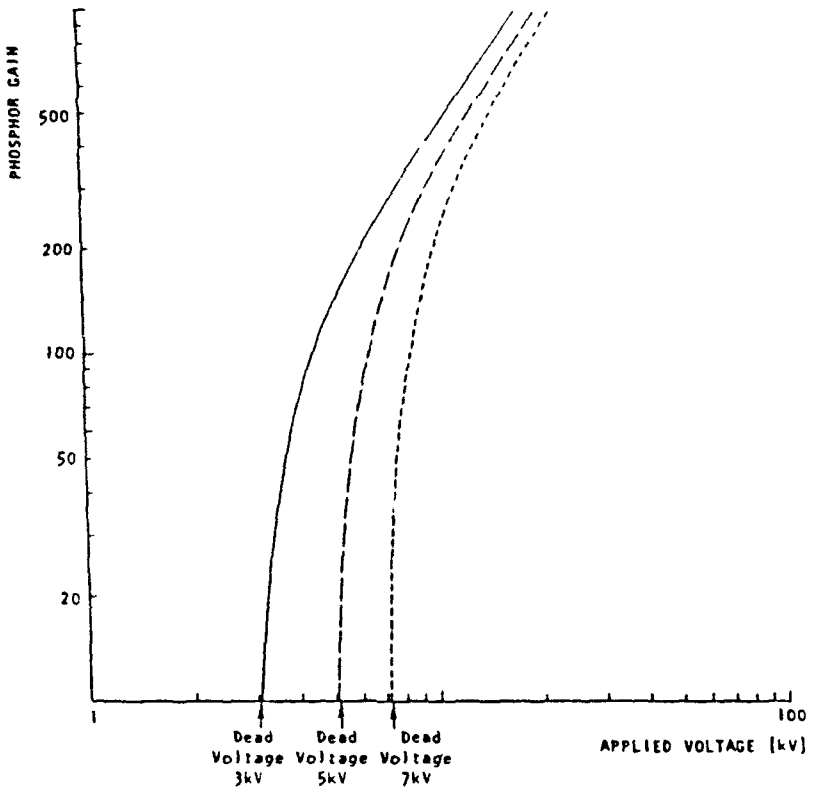

Fig. 10. Nonlinearity of P-20 phosphor gain attributable to dead voltage.

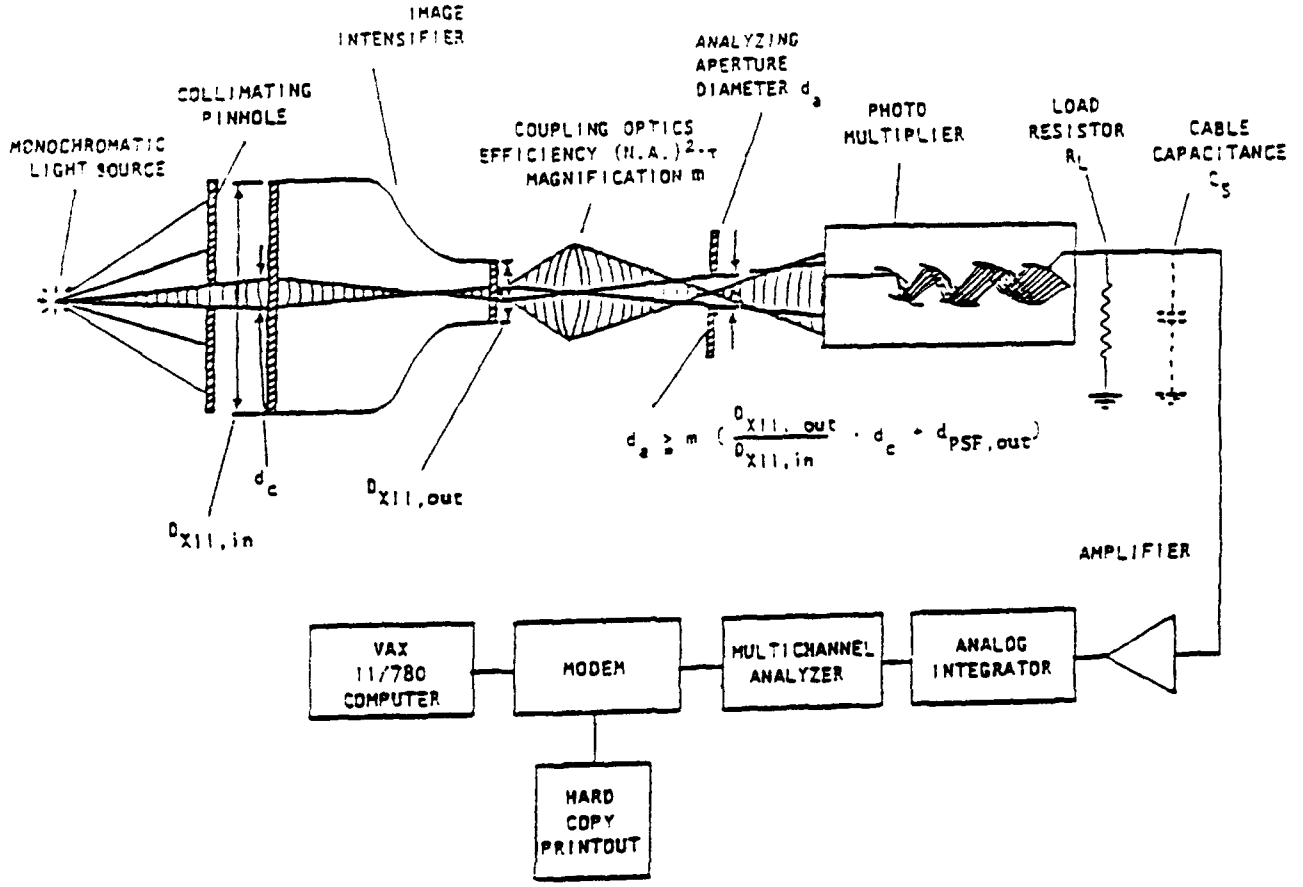

Fig. 11. Experimental setup for the measurement of single and multiple photon pulse-height distributions.

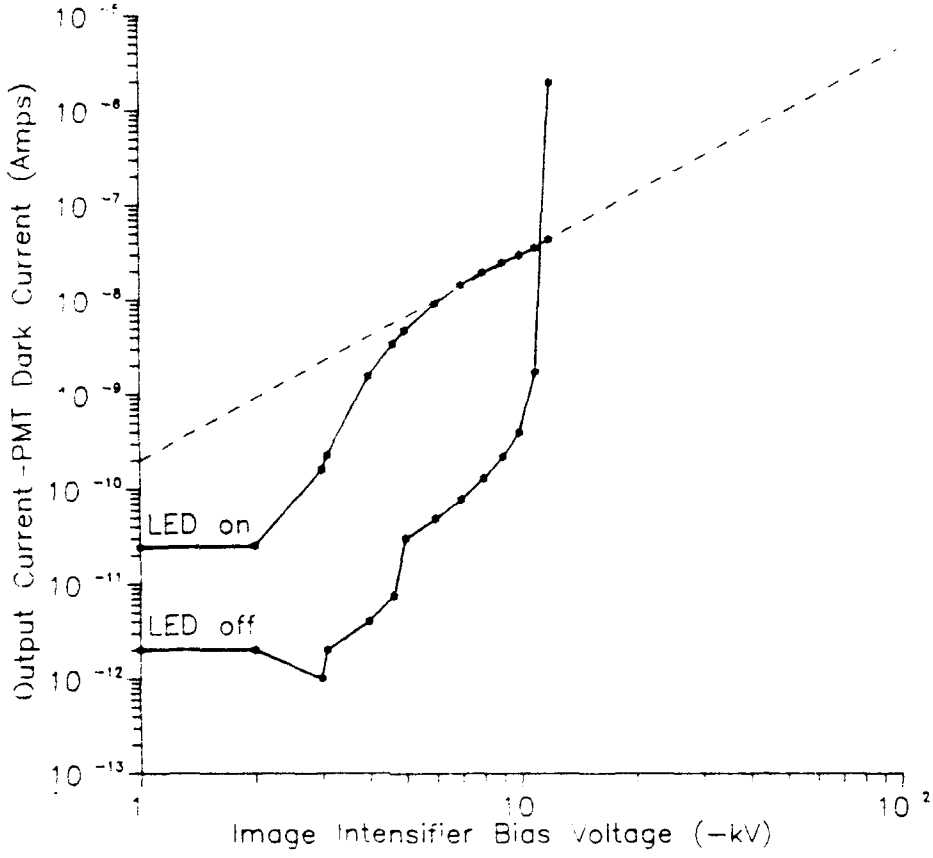

Fig. 12. Measured output of Varo image intensifier vs bias voltage.

Figure 12 is not exactly what one would expect from an image intensifier tube, particularly the measurements made at -11 and -12 kV bias voltages with the LED off.

From talking with Bill Flynt of Varo and from our own observations, we have come to the conclusion that this jump in output brightness at -11 and -12kV is most probably attributable to a field-emission point in the diode. We have observed, and Bill Flynt has confirmed for us, that field emission points may not be stable with respect to time or position, which could be why we did not observe the field emission during the time we had the LED on.

We also observed a sort of "hysteresis" effect with the field emission point, in that it came on above a certain bias voltage but turned off at a much lower bias voltage. It is plausible that during the LED "on" experiment, this "threshold" was never exceeded but during the LED "off" experiment, it inadvertently was, and when the bias voltage was reduced, the field emission point was still glowing. The data sheets included with this image intensifier tube indicate that the tube was damaged during testing and on observing the tube at high bias voltages, bright emission points could be seen.

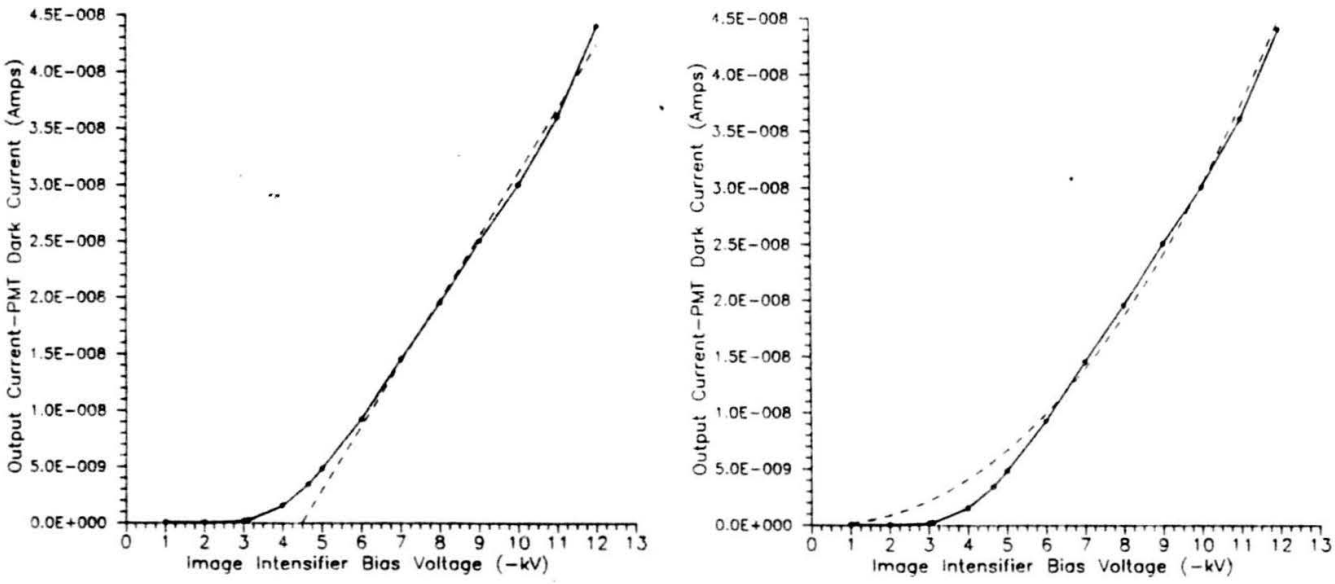

Fig. 13. Measured output of Varo image intensifier vs bias voltage with LED on: a) with a linear fit, b) with a power fit.

Extrapolating from the "LED on" curve in Fig. 12 down to the x-axis suggests a dead voltage of around -2kV (rather than the -4kV quoted by Varo). Furthermore, the portion of the curve which is emphasized by dashes suggests a value of 2.18 for n however the curve for "LED off" is completely different. On the other hand, the linear plot in Fig. 13a gives a dead voltage of -4.4kV. However, it is not clear whether a linear fit (Fig. 13a) or a power fit (Fig. 13b) should be used to best fit the data above -6kV. Therefore, it is not clear at this time what the correct dead voltage of the Varo image intensifier is.

Furthermore, it is not easy to understand why the curves in Fig. 12 for "LED on" and "LED off" are not "parallel." As is known from our own experience with PMTs,[9] dark and signal anode currents have practically the same dependence on the applied voltage. Both represent the voltage dependence of the gain and we would have expected no different for the intensifier's gain.

Looking at Fig. 13, we see a more traditional graph of output current (proportional to the number of photons leaving the phosphor) to bias voltage on a linear plot. From zero to -3 kV, we see no output from the tube and, by drawing a straight line through the remainder of the graph, we can estimate a dead voltage of about -4.4 kV. This value is a little high compared to information supplied by Varo, which claims a dead voltage of -4 kV. As explained above, until this bias voltage is reached, photoelectrons leaving the

photocathode do not have sufficient energy to traverse the aluminized screen and excite the phosphor. From -6 to -10 kV bias, the response follows a straight line, as one would expect if n=1, and above -10 kV, we see that the tube output is increasing in a slightly nonlinear manner which could indicate the field emission point described above.

References

1. Green, Sam, Ph.D., McDonnell-Douglas Corporation, private communication

2. Engstrom, Ralph W., Ph.D., RCA Photomultiplier Handbook, pg. 20, RCA Corporation, Lancaster, Pennsylvania, 1980.

3. Bar-Lev, Adir, Semiconductors and Electronic Devices, 2nd ed., pg. 447, Prentice Hall, New Jersey, 1984.

4. See reference 2.

5. Final Report for Contract #N66001-85-C-0118 to Naval Ocean Systems Center, University of Arizona, Optical Sciences Center, February, 1987.

6. RCA 8852 Photomultiplier Specifications Sheet, RCA Corporation, Lancaster, Pennsylvania.

7. Kazan, B. and M. Knoll, Electronic Image Storage, pg. 87, Academic Press, New York, 1968.

8. Ibid.

9. Roehrig, Hans, Ph.D., private communication

APPENDIX A

ANALYSIS WITH A SCANNING ELECTRON MICROSCOPE OF PHOSPHOR SCREENS

Final Scientific and Technical Report
April 14, 1987 (Covering period June 26 to September 30, 1986)
Prepared under Contract Number N66001-85-D-0203 for San Diego State University Foundation and the Naval Ocean Systems Center

Richard H. Cromwell
Steward Observatory
University of Arizona
Tucson, Arizona 85721

Introduction. We have carried out an investigation into the cause of why most phosphor screens fail to release a detectable burst of light in nearly half of the occasions where they are struck by a single photoelectron (reference 1). The present work differs from all of our earlier work, where previously we have directly measured the single electron counting efficiency in operating image intensifiers (reference 2). In this new study we have examined the very fine-scale cathodoluminescent properties of individual grains of P-20 phosphor powder using a scanning electron microscope (SEM). This technique allows observation for the very first time of the cathodoluminescent response of an area within a single phosphor grain that is at least one hundred times finer than an area resolvable by purely optical techniques. We have consequently been able to test many hypotheses concerning the cause of the disappointingly low counting efficiency of phosphor screens used in diode type image intensifiers.

Method. The electron microscope was instrumented so that three distinctly different types of images could be studied: 1) A standard "secondary electron" mode (SE), where images of the speciman are formed via collecting the secondary electrons emitted by the point being struck by a scanning electron beam; 2) A "cathodoluminescent" mode (CL_{FO}), where light emitted while one point is being struck by the electron beam is collected by a fiberoptic butted up against the output faceplate of the screen, and the resultant brightness of the image displayed on a CRT at that point is proportional to the amount of light emitted from the speciman; and 3) A second "cathodoluminescent" mode (CL_{EL}), identical to the CL_{FO} mode, only the light collected is that which is emitted toward the electron beam side of the screen, rather than that emitted through the output faceplate of the screen. The image displayed on the CRT of the SEM may be recorded on polaroid film. A second CRT displays the video waveform of the raster line currently being written on the first CRT. We have made video tapes using a standard video camera of both CRTs simultaneously. Slow-motion playback of the tapes later allow us to obtain photometric measurements of images shown on the first CRT through analysis of the waveform displayed on the second CRT. The figures accompanying this report are xerox copies of polaroid prints taken with the electron microscope. They are labeled according to which mode was used, namely SE, CL_{FO}, or CL_{EL}. In these pictures the black and shiny aluminum layer has been peeled away from the phosphor layer in order to see the grains.

Samples tested. SEM data have been recorded for many samples of P-20 phosphor screens that have been manufactured by Proxitronic using various modifications to their processing steps in an attempt to understand and improve the counting efficiency. The sample screens are described as follows:

1) all normal steps carried out,
2) settled phosphor only, no further steps,
3) settled phosphor, aluminized, lacquer baked out,
4) screen from previously operating tube, coarse grained, measured C.E. of operating tube = 42%,

5) screen from previously operating tube, 2x thickness, no electron scrubbing, measured C.E. of operating tube = 50%.
6) screen from previously operating tube, 4x thickness, measured C.E. of operating tube = 70%.

Following a preliminary SEM analysis of the above screens, Proxitronic then prepared a second set of samples as follows:

1) settled phosphor, 1.5x thickness, standard lacquer thickness, standard aluminum layer, 420°C lacquer burnout, nothing more (i.e., no black layer, no electron scrub, no other bake).
2) like (1), only without lacquer burnout step.
3) like (1), only with twice lacquer thickness.
4) like (1), only with half lacquer thickness.
5) like (1), only with double thickness of aluminum.
6) like (1), only with black layer and with half of screen electron scrubbed and other half not.

Results from preliminary SEM analysis.

1) In the standard thickness screens (0.7 mg/cm^2), the SEM images taken in the two cathodoluminescent modes (CL_{EL} and CL_{FO}) show that voids, or holes, in the screens constitute roughly 10% of the total projected area of a screen. This directly accounts for a 10% loss in counting efficiency for such screens. In earlier optical microscope examinations of screens, we were unable to accurately determine the size of these holes, but suspected they could be large enough to explain the nearly 50% loss in counting efficiency that is typical of screens. The electron microscope images conclusively refute this large of an effect. The electron microscope also clearly shows that 2x and 4x phosphor thickness screens are too thick, and that a 1.5x thickness is optimum for reducing the area of holes to a negligible level (i.e., less than 1% of the screen surface). Making screens thicker than 1.5x creates the undesirable effect of reduced gain via absorption of light by underlying grains. This is dramatically revealed in CL_{FO} pictures of the 1x, 1.5x, 2x and 4x screens.

2) The cathodoluminescent images have revealed that there exist a few grains that are virtually dead and that other grains are of very reduced efficiency. This is in marked contrast to our findings using the industry-accepted technique of examining screens by shining UV light on them and by inspecting the luminescing grains with an optical microscope. Using this optical method we have never detected even one dead grain. Nonetheless, the number of totally dead grains revealed by the SEM is in fact quite negligible (less than 1%).

3) Some intensifier manufacturers have cautioned against the use of the very tiniest grains, reportedly observing that such grains are dead. In all our SEM tests, there is no evidence that the smallest grains (0.5 micron diameter) have a different cathodoluminescent efficiency than the largest grains (4 microns diameter).

4) At least 80% of all grains of a screen that may be directly viewed by the electron microscope may be classed as having a "typical cathodoluminescent structure". The typical grains are described as follows:

a) They appear to cathodoluminesce over 100% of their surface exposed to electrons, shown in both CL_{FO} and CL_{EL} modes.

b) They appear uniformly sensitive (to better than $\pm$10%) over their entire surface, and contain no apparent super-sensitive, or insensitive, spots or shells or cores shown in both CL_{FO} and CL_{EL} modes.

c) The peak-to-peak variation in response from one of these "typical" grains to another "typical" grain <u>on the same screen</u> is less than $\pm$15%.

5) Besides these typical grains, every screen contains a small percentage of grains (1-10%) that are dead, or have small dead areas, or have small high-sensitivity areas, etc. Although interesting, these grains appear to have very little effect on the overall performance characteristics of a screen.

6) In the early phases of our study, it appeared as though most of the grains in the top layer (i.e., the grains nearest the aluminum) were of reduced cathodoluminescent efficiency, even in the CL_{EL} images. However, further analysis reveals this is a false impression and is simply due to an optical effect between the top grains and the CL_{EL} sensor. Note: In the CL_{FO} mode, the top grains are always darker because their light is absorbed by lower grains situated between them and the CL_{FO} sensor.

7) Another property discovered in the early phases of our study is that grains that are excavated from the screen surface are roughly 50% brighter than the remaining undisturbed grains, when observed in the CL_{EL} mode. This property, along with the earlier suspected low-efficiency of top grains mentioned in item (6) above, led us to suspect that the excavated grains were predominantly from the bottom layer of screen and that this bottom layer had been protected from a manufacturing process that had selectively reduced the sensitivity of the top layer grains, but not the bottom grains.

<u>Results from second set of screen samples.</u> The second set of samples manufactured by Proxitronic (see list given in section, "Samples tested") were prepared in order to allow us to test specific processing steps suspected of destroying the top layer of grains more than the bottom layer. Any step that selectively destroys the top grains would normally go undetected in screen quality-control test procedures performed during normal manufacture because the top layer is hidden from view via the aluminum layer of the screen. Recognizing this, we were very encouraged by our initial SEM results that the second test samples could identify the cause of low counting efficiency. In the summary of results that follows, we discover that the earlier interpretation of screens containing a partially destroyed top layer of grains is wrong and, indeed, that no screen

manufacturing process thus far examined appears to damage the grains.

1) In our preliminary SEM analysis we had found what appeared to be a general progression in the number of damaged grains with each successive screen processing step. However, results from the additional samples and repeated and improved tests of the earlier samples have revealed that the earlier suspicians are unfounded, and that the proper explanation lies in certain optical effects of the CL_{EL} sensor, as already mentioned in items (6) and (7) of the section "Results from preliminary SEM analysis." The important new results follow.

2) The ratio of CL_{EL} signal from the average gray level of a screen to the signal from the very few brightest grains is found to be virtually a constant for all screens examined, and is 0.68 ± 0.02. This includes screens ranging from a settled-phosphor-only through a 4x-thickness-screen removed from a previously operating tube. Thus, no processing step was found to influence this ratio. (Earlier, we had thought a steady progression in this ratio existed, but now we realize such evidence was incorrectly influenced by extraneous optical effects of particular samples.)

3) The number of dead and partially destroyed grains in both the top and bottom layers of a screen seems to be rather similar among all samples of screens examined, <u>including</u> even the sample without lacquer burnout and the settled phosphor only sample. (Again, earlier we had been misled in this conclusion by various optical effects and by the effects of variable electron voltages applied in some of the early tests.)

4) In repeated attempts, we finally were successful in scraping away with a razor blade only the top layer of grains from a screen. In the resulting exposed bottom layer of grains, there was no detectable difference in the CL_{EL} signal strength from these grains or the surrounding undisturbed top-layer grains.

5) By studying CL_{EL} images of many different screen samples where grains had been purposely excavated from the screen layer, we discovered that the reason such grains appeared 50% brighter than all others was due to an optical effect with the CL_{EL} sensor, and not to an inherent high efficiency of the excavated grains. This discovery was ultimately responsible for our determining that the dark-core/bright-halo appearance of the topmost grains was also due to an optical effect. Earlier, we had misinterpreted this appearance as due to partial damage of top grains.

6) In the sample where half of the screen was electron scrubbed and the other half was not, there was absolutely no detectable difference in the cathodoluminescent efficiency or structure between the two halves.

Conclusions and recommendations. The most clearcut result of this SEM investigation is that phosphor screens manufacatured by Proxitronic are slightly too thin for optimum counting efficiency (and we suspect this is likely to be true for screens manufactured by others as well). There is no SEM evidence that grain size, within the size range of the Riedel de Haen powder examined here, influences the counting efficiency of a screen. (However, we should note that there is a modest suggestion in our counting efficiency measurements in operating intensifiers that, if indeed there is a measurable difference, small grains may perform better than larger ones.) A finite number of dead or reduced-sensitivity grains are present in all screens, but the percentage is negligible. Finally, there is no evidence that any of the screen processing steps carried out at Proxitronic damage or otherwise alter the cathodoluminescent properties of the original phosphor powder.

Therefore, although we undertook this SEM project with considerable enthusiasm that we would be able to identify one or more phosphor screen processing steps that were damaging the cathodoluminescence of the original phosphor powder, it now seems clear that none of the earlier plausible candidates are at fault. Having eliminated a number of likely explanations, of course, means that we simply must search elsewhere for the true cause. At this moment, the most likely explanation would seem to be that there exist one or more steps employed by the manufacturer of the phosphor powder proper (e.g. at Riedel de Haen) that is at fault. We earlier had dismissed this possibility on the basis that nearly all intensifiers we have analysed, from a variety of tube and phosphor manufacturers, have a similar, low counting efficiency. Moreover, the one intensifier manufacturer that has produced phosphors of high counting efficiency at least some of the time (although not all of the time), is Varo, and Varo claims to have used the same supplier of phosphor as the present Proxitronic powder, Riedel de Haen.

Toward learning what creates a high counting efficiency phosphor, we plan to carry out the following steps in the future:

1) Examine with the SEM a phosphor screen that has been dismantled from a previously operating intensifier that we have measured to have a high counting efficiency (selected from various reject Varo tubes we presently have). To date, we have examined with the SEM only one Varo screen, and it was from a tube of unknown counting efficiency.

2) Measure the counting efficiency of a Proxitronic intensifier having a brushed-on P-20 phosphor screen, instead of their standard settled phosphor screen.

3) Measure the counting efficiency of ITT intensifiers having P-47 fast-response phosphors.

4) Measure the counting efficiency of Proxitronic intensifiers having X-3 fast-response phosphors.

5) Discuss our results with producers of raw phosphor powder and collaborate with same in producing a high counting efficiency phosphor.

References.

1) The Lost Photon Problem in Image Intensifiers (R.H. Cromwell) 1984, Bulletin American Astronomical Society, 16, No. 4, 904 (Abstract). Steward Observatory Preprint No. 565 (Full Paper).

2) Toward Solving the Lost Photon Problem in Image Intensifiers (R.H. Cromwell) 1986, Instrumentation in Astronomy VI, David L. Crawford, Editor, Proceedings of the SPIE, 627, 610.

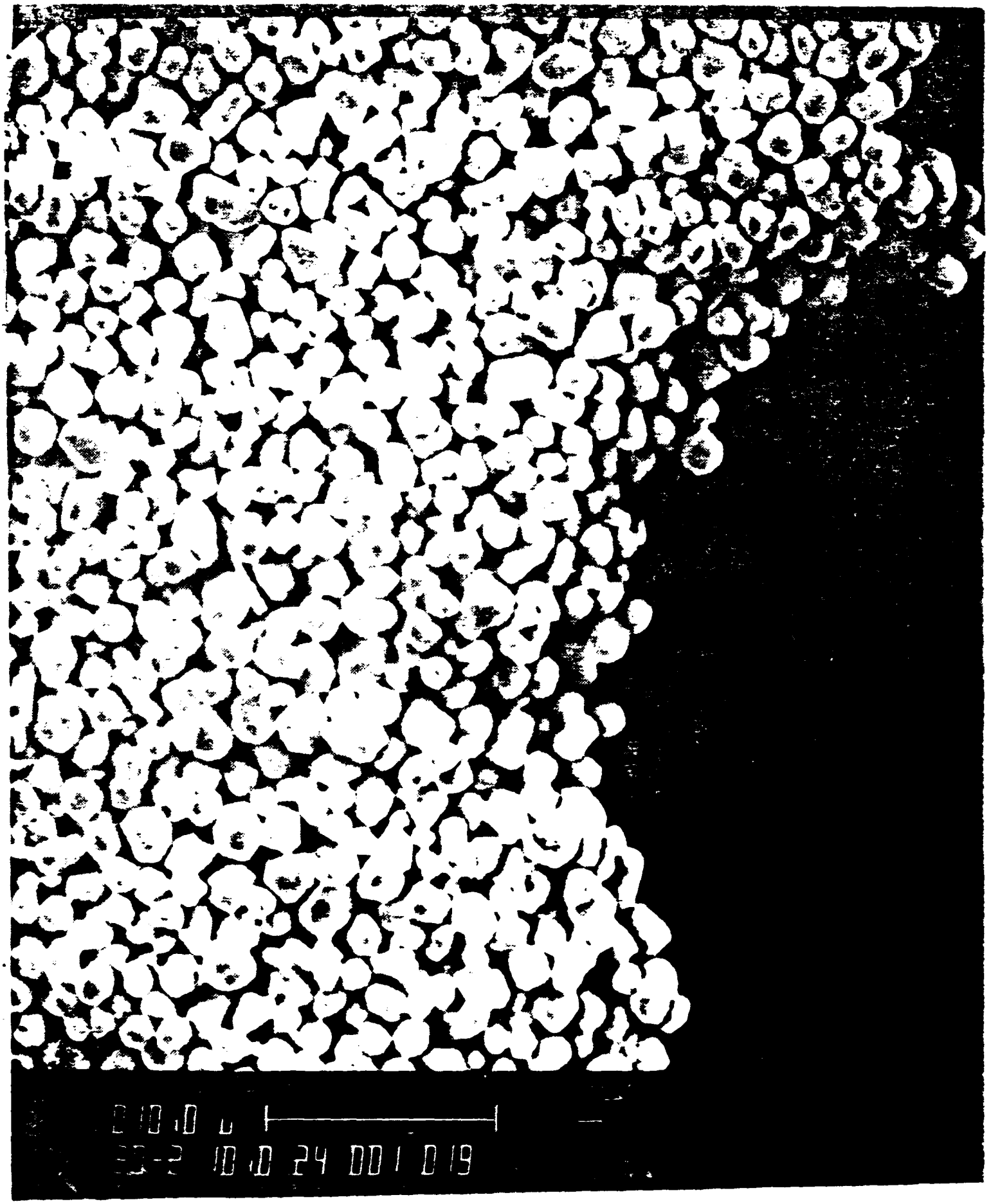

Figure 1. SE image of 2x thickness screen from a previously operating intensifier.

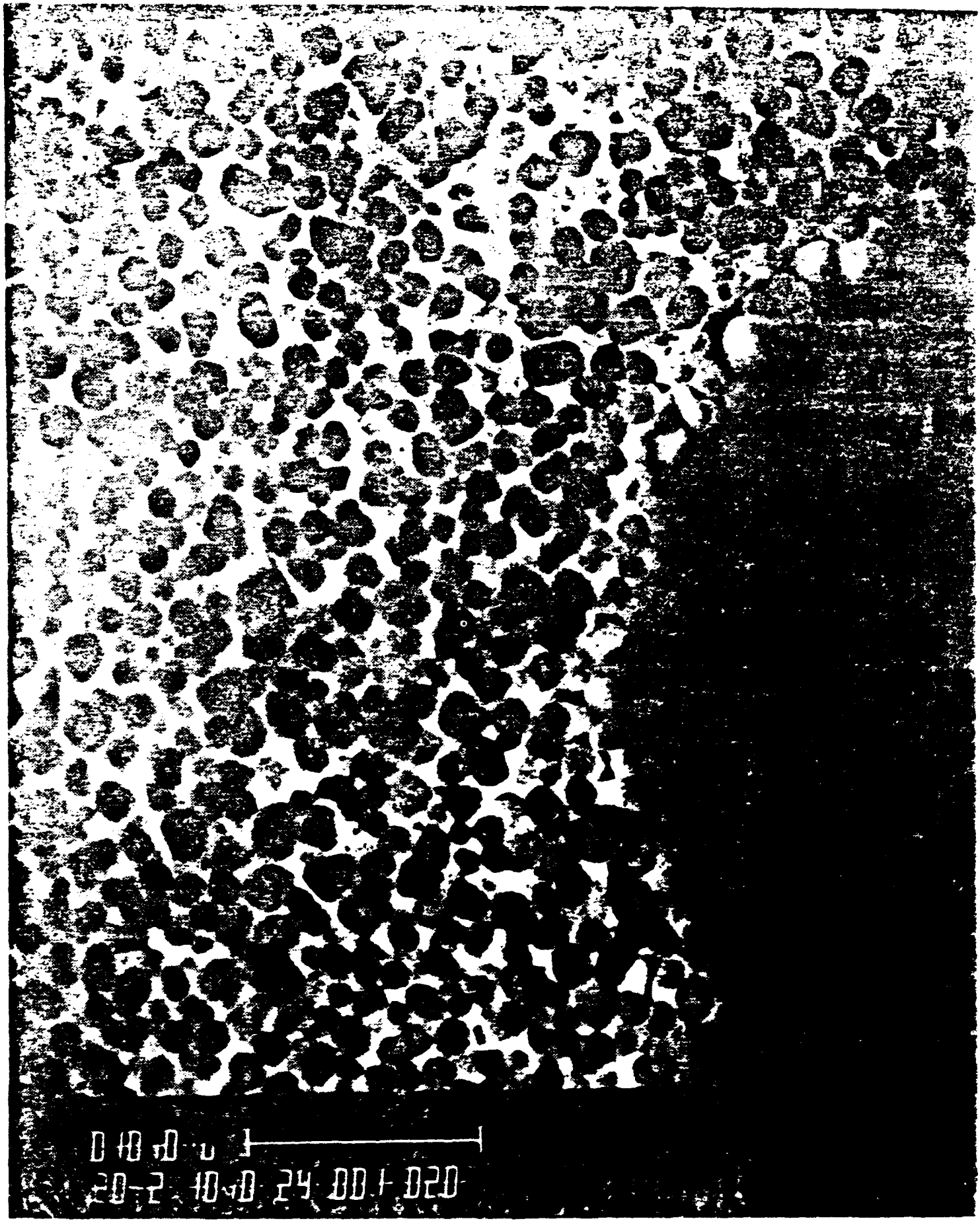

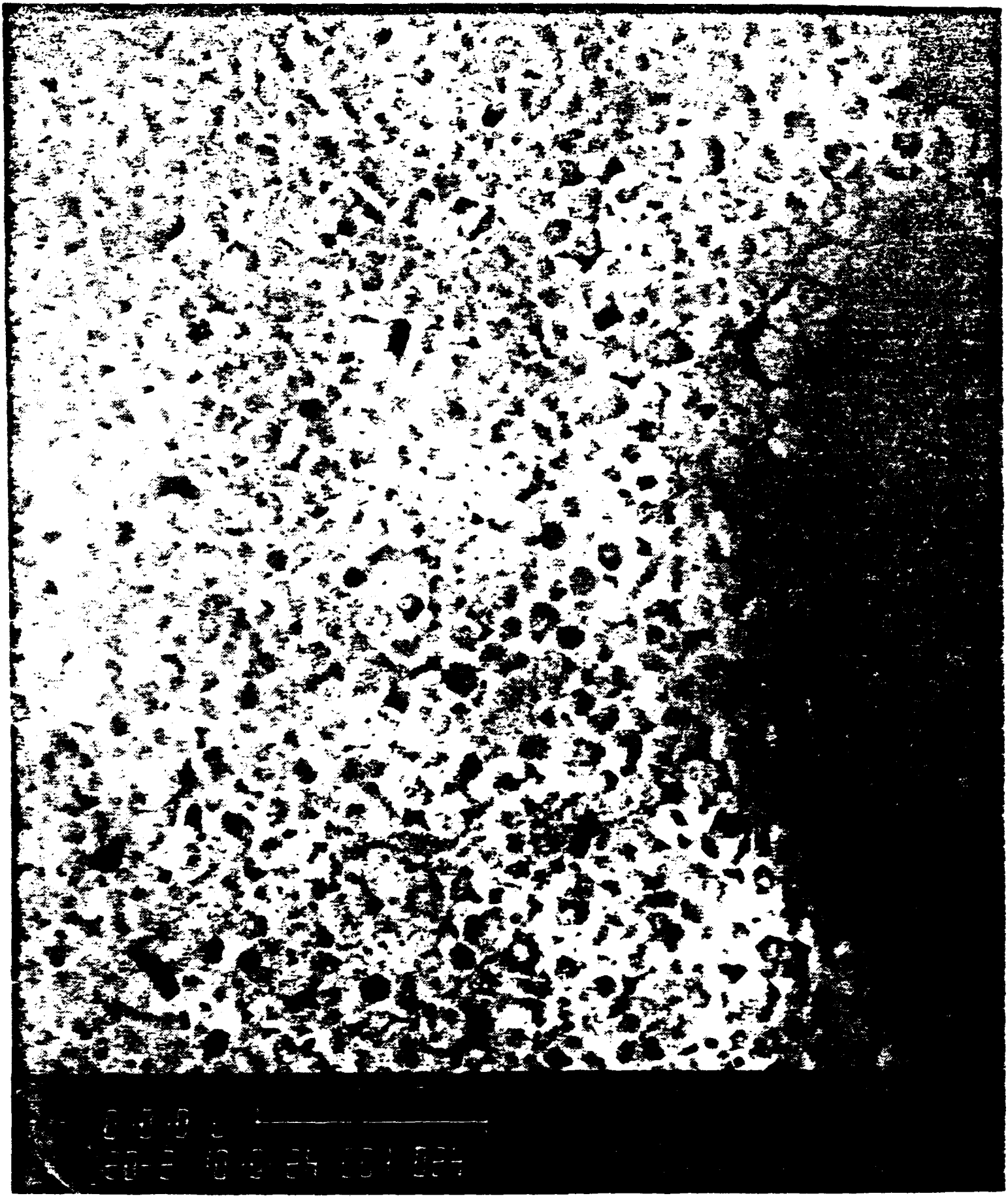

Figure 3. CL$_{ET}$ image of same region as shown in Figures 1 and 2. There are very few dead grains and virtually no voids in this 2x thick screen. The appearance that some of the top-most grains cathodoluminesce with a somewhat dark core and bright halo is due to optical effects of the CL$_{ET}$ sensor, and is not a true

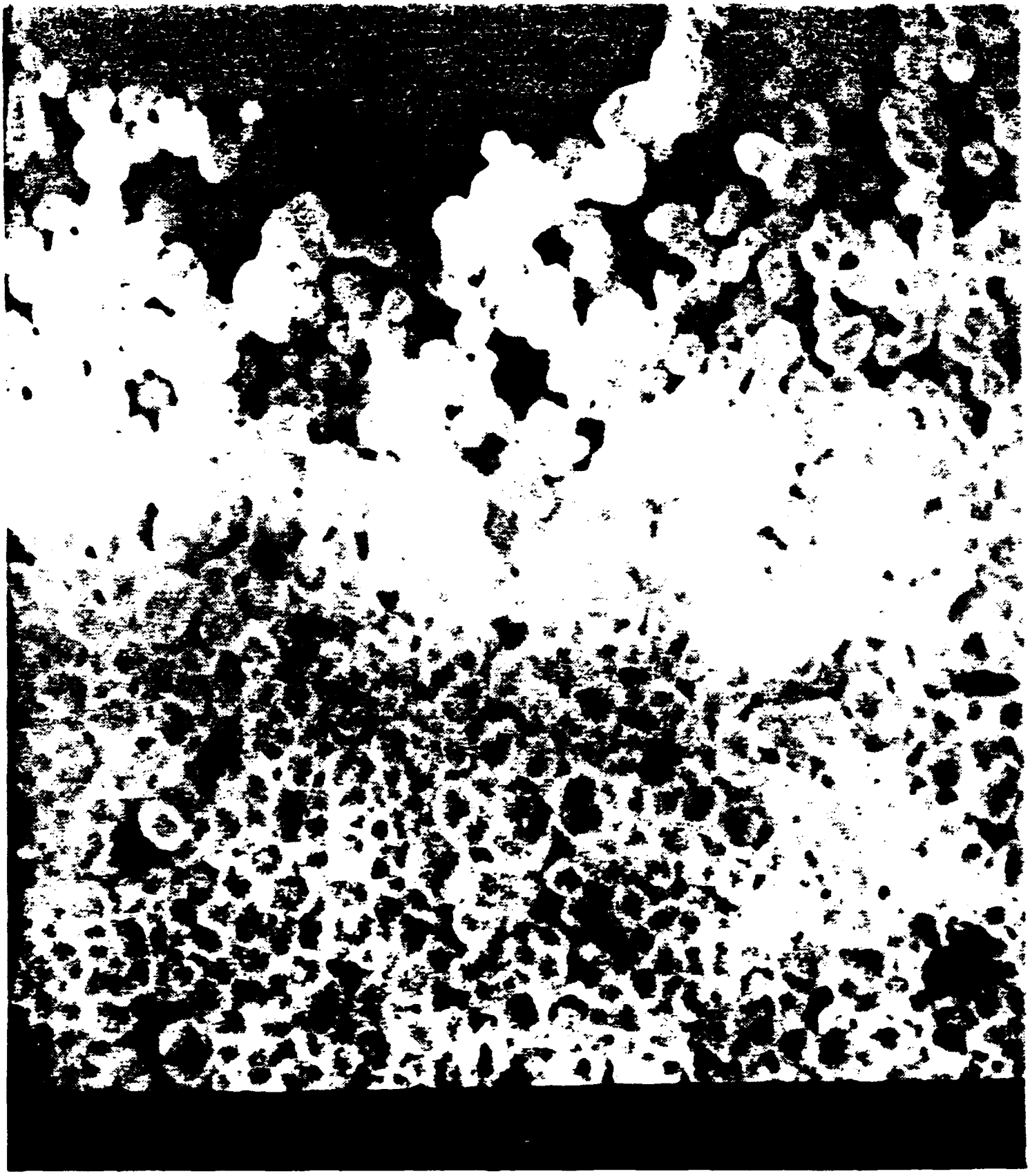

Figure 4. CL_{e_1} image of 1.5x thickness screen prepared without the lacquer burnout step that normally follows the aluminizing process. The grains of this screen are found to have virtually identical cathodoluminescent properties to the grains of fully processed screens that have been dismantled from previously operating intensifiers. The exceptionally bright clumps of grains in this photograph are grains that have been excavated from the screen. Their extra brightness arises from optical effects of the CL_{e_1} sensor, and is not an inherent property of the grains.

Figure 5. CL$_{2}$ image of screen that has had half of its surface electron scrubbed (that half above the three scratch marks devoid of phosphor) and the other half not electron scrubbed. There is no detectable difference in the cathodoluminescent properties between the two halves.

Approved for public release:
distribution is unlimited.

The views and conclusions contained in this report are those of the authors and should not be interpreted as representing the official policies, either expressed or implied, of the Naval Ocean Systems Center or the U.S. Government.